ISSN 1674-1056
http://cpb.iphy.ac.cn
http://iopscience.iop.org/cpb
中国物理 B
Chinese Physics
中国物理 Chinese Physics B

Atmospheric N_2O gas detection based on an inter-band cascade laser around 3.939 μm

Chun-Yan Sun(孙春艳)[1,2,3], Yuan Cao(曹渊)[1,2], Jia-Jin Chen(陈家金)[1], Jing-Jing Wang(王静静)[1,2], Gang Cheng(程刚)[1,2], Gui-Shi Wang(王贵师)[1], Xiao-Ming Gao(高晓明)[1]

Citation: Chin. Phys. B . 2020, 29(1): 010704 . **doi:** 10.1088/1674-1056/ab5ef6
Journal homepage: http://cpb.iphy.ac.cn; http://iopscience.iop.org/cpb

What follows is a list of articles you may be interested in

Highly-sensitive NO, NO_2, and NH_3 measurements with an open-multipass cell based on mid-infrared wavelength modulation spectroscopy

Xiang Chen(陈祥), Chen-Guang Yang(杨晨光), Mai Hu(胡迈), Jian-Kang Shen(沈建康), Er-Chao Niu(牛二超), Zhen-Yu Xu(许振宇), Xue-Li Fan(范雪丽), Min Wei(魏敏), Lu Yao(姚路), Ya-Bai He(何亚柏), Jian-Guo Liu(刘建国), Rui-Feng Kan(阚瑞峰)

Chin. Phys. B . 2018, 27(4): 040701 . **doi:** 10.1088/1674-1056/27/4/040701

Absorption linewidth inversion with wavelength modulation spectroscopy

Yue Yan(颜悦), Zhenhui Du(杜振辉), Jinyi Li(李金义), Ruixue Wang(王瑞雪)

Chin. Phys. B . 2018, 27(2): 024205 . **doi:** 10.1088/1674-1056/27/2/024205

Wavelength modulation spectroscopy for measurements of gas parameters in combustion field

Dong-Sheng Qu(屈东胜), Yan-Ji Hong(洪延姬), Guang-Yu Wang(王广宇), Hu Pan(潘虎)

Chin. Phys. B . 2017, 26(6): 064207 . **doi:** 10.1088/1674-1056/26/6/064207

Daily variation of radon gas and its short-lived progeny concentration near ground level and estimation of aerosol residence time

M Mohery, A M Abdallah, A Ali, S S Baz

Chin. Phys. B . 2016, 25(5): 050701 . **doi:** 10.1088/1674-1056/25/5/050701

Theoretical analysis of stack gas emission velocity measurement by optical scintillation

Yang Yang, Dong Feng-Zhong, Ni Zhi-Bo, Pang Tao, Zeng Zong-Yong, Wu Bian, Zhang Zhi-Rong

Chin. Phys. B . 2014, 23(4): 040703 . **doi:** 10.1088/1674-1056/23/4/040703

Atmospheric N_2O gas detection based on an inter-band cascade laser around 3.939 μm*

Chun-Yan Sun(孙春艳)[1,2,3], Yuan Cao(曹渊)[1,2], Jia-Jin Chen(陈家金)[1], Jing-Jing Wang(王静静)[1,2], Gang Cheng(程刚)[1,2], Gui-Shi Wang(王贵师)[1,†], and Xiao-Ming Gao(高晓明)[1]

[1] *Anhui Institute of Optics and Fine Mechanics, Chinese Academy of Sciences, Hefei* 230031, *China*
[2] *University of Science and Technology of China, Hefei* 230031, *China*
[3] *Huainan Normal University, Huainan* 232001, *China*

(Received 10 August 2019; revised manuscript received 22 October 2019; accepted manuscript online 5 December 2019)

N_2O is a significant atmospheric greenhouse gas that contributes to global warming and climate change. In this work, the high sensitivity detection of atmospheric N_2O is achieved using wavelength modulation spectroscopy (WMS) with an inter-band cascade laser operating around 3.939 μm. A LabVIEW-based software signal generator and software lock-in amplifiers are designed to simplify the system. In order to eliminate the interference from water vapor, the detection was performed at a pressure of 0.1 atm (1 atm = 1.01325×10^5 Pa) and a drying tube was added to the system. To improve the system performance for long term detection, a novel frequency locking method and $2f/1f$ calibration-free method were employed to lock the laser frequency and calibrate the power fluctuations, respectively. The Allan deviation analysis of the results indicates a detection limit of ∼ 20 ppb (1 ppb = 1.81205 μg/m^3) for a 1 s integration time, and the optimal detection limit is ∼ 5 ppb for a 40-s integration time.

Keywords: wavelength modulation spectroscopy, inter-band cascade laser, frequency locking, nitrous oxide (N_2O)

PACS: 07.88.+y, 42.87.–d, 42.72.Bj, 33.20.Lg **DOI:** 10.1088/1674-1056/ab5ef6

1. Introduction

Nitrous oxide (N_2O) is one of the most significant atmospheric greenhouse gases contributing to global warming and climate change. It participates in atmospheric chemical reactions in the atmosphere and is a primary scavenger of stratospheric ozone.[1] N_2O is about 300 times more potent at warming the atmosphere per unit weight than CO_2, and its concentration in the planet boundary layer has been continuously increasing due to anthropogenic in recent years.[2,3] Consequently, high precision measurement of N_2O is necessary to determine the emission sources and concentration level, which may lead to a better understanding of global warming and climate change.[4,5]

Over the last decades, tunable diode laser absorption spectroscopy (TDLAS)[6,9] has become an important optical method for trace gas detection. With the development of quantum cascade (QC) and inter-band cascade (IC)[10,11] lasers in the 3 μm–12 μm spectral region, where many trace gases have strong fundamental ro-vibrational bands, the applications of mid-infrared TDLAS for trace gas detection become feasible. Other techniques, such as quartz enhanced photo-acoustic spectrum (QEPAS), have also benefitted from the development of mid-infrared lasers, and have proven to be a powerful candidate for trace gas detections.[12]

When the tunable laser works in the free running mode, the center frequency may drift with time, which results in system instability. Normally, a feedback servo loop is employed,[13–16] using odd harmonic signals from a reference cell, to stabilize the laser emission frequency. Recently, a scanned frequency locking method without reference absorption cell is reported,[17,18] where the center spacing between two second harmonic peaks is employed as a frequency locking reference. However, this method is only suitable when the signal to noise ratio is high. Consequently, a more adaptive method is needed for general applications. Another effective way to improve the system stability is eliminating the fluctuations of the laser intensity. A proved $2f/1f$ calibration-free method was applied in the present work.[19,20]

In this paper, a TDLAS based N_2O measurement system is demonstrated. For simplifying the system, a LabVIEW-based software signal generator and software lock-in amplifiers are designed combining a 3.939-μm ICL laser. In addition, for improving the system performance for long term detection, a novel correlation frequency locking method is recommended. This article is organized as follows: the first part is an introduction of the method and system details. Then, the results obtained in a static absorption cell and atmospheric measurements are discussed. Finally, the detection limit of the system is analyzed by the Allan deviation method.

*Project supported by the National Key Research and Development Program of China (Grant Nos. 2018YFC0213304, 2017YFC0209703, and 2016TFC0303900).

†Corresponding author. E-mail: gswang@aiofm.ac.cn

© 2020 Chinese Physical Society and IOP Publishing Ltd

2. Methods and system details

2.1. Theory of wavelength modulation spectroscopy

When a sinusoidal wave with a frequency f is superimposed to the laser supply, the current, the output frequency and the corresponding intensity $I_0(t)$ of the laser can be written as

$$\nu(t) = \overline{\nu}(t) + a\cos(\omega t), \tag{1}$$

$$I_0(t) = \bar{I}_0[1 + i_0\cos(\omega t + \psi_1) + i_2\cos(2\omega t + \psi_2)], \tag{2}$$

where $\bar{\nu}$ and $\bar{I}_0$ are the center frequency of the laser and the average light intensity at the center frequency, a is the modulation amplitude (in unit cm^{-1}), $\omega = 2\pi f$ is the angular frequency, I_0 is the linear laser intensity modulated (IM) amplitude, i_2 is the nonlinear IM amplitude, ψ_1 is the phase shift of the ratio of linear frequency modulation (FM) to laser intensity modulation (IM), and ψ_2 is the phase shift of the nonlinear FM to IM ratio.

According to the Beer–Lambert law, the transmitted light intensity $I(t)$ can be expressed as

$$I(t) = I_0(t)\exp(-\alpha(\upsilon)). \tag{3}$$

For an optically thin sample (typically $\alpha(\nu) < 0.1$), the transmittance can be approximately described by the following formula

$$\tau(\overline{\nu} + a\cos\omega t) \approx 1 - \alpha(\overline{\nu} + a\cos\omega t). \tag{4}$$

The absorbance coefficient $\alpha(\nu)$ in Eq. (4) can be expanded by a Fourier cosine series as

$$\alpha(\overline{\nu} + a\cos\omega t) = -\sum_{k=0}^{\infty} H_k(\overline{\nu}, a)\cos(k\omega t). \tag{5}$$

In wavelength modulation spectroscopy (WMS), the second harmonic signal[21] is obtained by demodulating the detection signal using a lock-in amplifier at a frequency of 2ω, and the corresponding X and Y components are described by Eqs. (6) and (7), respectively

$$X_{2f} = \frac{G\bar{I}_0}{2} = \left[H_2 + \frac{i_0}{2}(H_1 + H_3)\cos\psi_1 + i_2\left(1 + H_0 + \frac{H_4}{2}\right)\cos\psi_2\right], \tag{6}$$

$$Y_{2f} = -\frac{G\bar{I}_0}{2} = \left[\frac{i_0}{2}(H_1 - H_3)\sin\psi_1 + i_2\left(1 + H_0 - \frac{H_4}{2}\right)\sin\psi_2\right]. \tag{7}$$

The background component of the second harmonic signal can be measured by filling the sample cell with pure N_2, and removing the no absorption signal from X and Y to obtain the second harmonic component S_{2f} that is related to the absorption:

$$S_{2f} = \sqrt{X_{2f}^2 + Y_{2f}^2} = \frac{G\bar{I}_0}{2}\left\{\left[H_2 + \frac{i_0}{2}(H_1 + H_3)\cos\psi_1 + i_2\left(H_0 + \frac{H_4}{2}\right)\cos\psi_2\right]^2 + \left[\frac{i_0}{2}(H_1 - H_3)\sin\psi_1 + i_2\left(H_0 - \frac{H_4}{2}\right)\sin\psi_2\right]^2\right\}. \tag{8}$$

Then, the amplitude of the S_{2f} signal still depends on the detection gain G and the average laser intensity $\bar{I}_0$. The amplitude of the first harmonic ($1f$) signal can also be obtained by digital phase locking as

$$S_{1f} = \frac{G\bar{I}_0}{2}\left\{\left[H_1 + i_0\left(H_0 + \frac{H_2}{2}\right)\cos\psi_1 + \frac{i_2}{2}(H_1 + H_3)\cos\psi_2\right]^2 + \left[i_0\left(H_0 - \frac{H_2}{2}\right)\sin\psi_1 + \frac{i_2}{2}(H_1 - H_3)\sin\psi_2\right]^2\right\}. \tag{9}$$

Finally, the detection gain factor G and the average laser intensity $\bar{I}_0$ can be eliminated by considering $2f/1f$ and the normalized signal is proportional to the gas concentration:

$$C_{2f/1f} \propto \frac{S_{2f}}{S_{1f}} \approx \frac{1}{i_0}\left\{\left[H_2 + \frac{i_0}{2}(H_1 + H_3)\cos\psi_1 + i_2\left(H_0 + \frac{H_4}{2}\right)\cos\psi_2\right]^2 + \left[\frac{i_0}{2}(H_1 - H_3)\sin\psi_1 + i_2\left(H_0 - \frac{H_4}{2}\right)\sin\psi_2\right]^2\right\}. \tag{10}$$

2.2. System details

2.2.1. Sensor design

The schematic diagram of the N_2O gas detection system is shown in Fig. 1. A DFB ICL (Nanoplus) centered at 3.9396 μm was used to probe the N_2O absorption line around 2539.3 cm^{-1}. The wavelength scanning and modulation was implemented by applying a semi-modulated triangle waveform made of a 2-V 20-Hz triangle scanning and a 0.5-V 10-kHz sinusoidal dither, to the laser controller (ILX Lightwave, LDC-3724B). After passing through a 100-m optical path multiple-pass cell (MPC, with a basal length of 50 cm) equipped with a pressure monitor and controller, the output beam was focused onto a fast TE-cooled mercury cadmium telluride (MCT) infrared detector (PVI-4TE-5, Vigo Systems). Subsequently, the output signal is acquired at a sampling rate of 400 kHz via a laptop equipped with a DAQ card (National Instruments, USB-6366) for data storage and further processing.

During the data processing, the rising edge signal is demodulated by the software lock-in amplifier to obtain the corresponding harmonic signals and the falling edge signal is processed to obtain the absolute concentration information. In order to lock the laser frequency, a software proportional integral derivative (PID) based feedback server loop is designed to adjust the laser working current through a USB cable, where the error control signal is calculated by using a correlation algorithm.

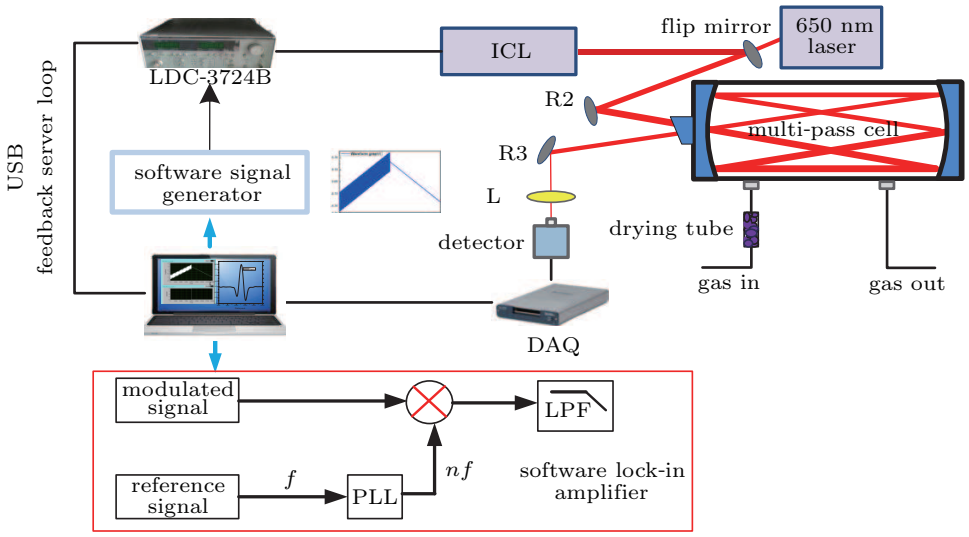


Fig. 1. Schematic diagram of the ICL sensor and the N_2O gas detection system. ICL: inter-band cascade laser, DAQ: data acquisition, LPF: low-pass filter, PLL: phase lock loop.

2.2.2. Selection of spectral line

In TDLAS based applications, choosing the proper absorption lines is critical. The absorption line is mainly selected from the following four points: (i) an appropriate band; (ii) strong spectral line intensity; (iii) the selected spectral line should meet the wavelength range of matured laser and detector; (iv) minimum interference from other gases, especially water vapor, should be avoided. However sometimes, the interference from other molecules cannot be avoided. A possible solution is to perform the measurement at a low pressure or using multi-peaks fitting method.

In the present work, two absorption lines of N_2O and water vapor near 2589.3 cm^{-1} were chosen for testing, and the low pressure method is considered for isolating the N_2O spectra from water vapor. Figure 2 shows the calculated absorption according to the HITRAN 2016 database.[22] The absorption features at 0.1 atm and 1 atm are shown in Figs. 2(a) and 2(b), respectively. Figure 2(a) shows that the contribution of the water vapor can be neglected at 0.1 atm, which validates using the WMS method to detect the atmospheric N_2O concentration at low pressures.

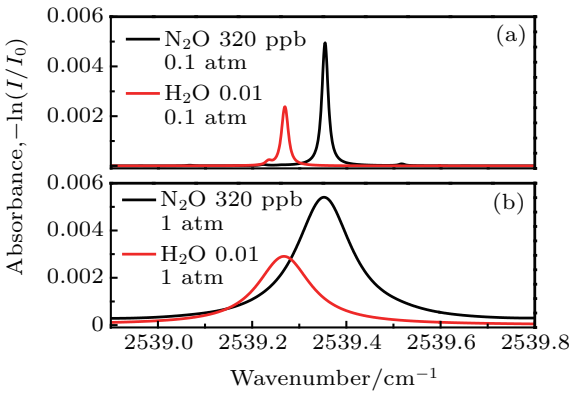


Fig. 2. Comparison of the N_2O and H_2O absorption spectra at a pressure of (a) 0.1 atm and (b) 1 atm.

2.2.3. Signal processing

(I) LabVIEW-based software signal generator

In order to simplify the system, a software signal generator is designed using the LabVIEW environment and a DAQ card that can generate arbitrary waveforms for specific applications. Figure 3 shows the semi-modulated triangle scan waveform and the TTL trigger signal used in this study. By using such a scan signal, the wavelength modulation spectrum and the direct absorption spectrum can be obtained simultaneously, where the rising edge is demodulated by a software lock-in amplifier to obtain the corresponding harmonic signals, and the falling edge is processed to obtain the absolute concentration information.

(II) LabVIEW-based software lock-in amplifier

A software lock-in amplifier is also designed in the LabVIEW environment to demodulate the harmonic signals. The n-th harmonic signal demodulated by the software digital lock-in amplifier can be expressed as

$$\mathrm{WMS}_{nf} = \sqrt{[I(t)\sin(2\pi n f_m)\otimes \mathrm{LPF}]^2 + [I(t)\sin(2\pi n f_m)\otimes \mathrm{LPF}]^2}, \tag{11}$$

where $I(t)$ is the modulated intensity and LPF represents a low-pass filter. The schematic diagram of the LabVIEW-based software lock-in amplifier is shown in Fig. 4. It mainly consists of a multiplier, a low pass filter, and an optional phase lock loop (PLL). It should be noted that since the scan signal is synthesized by the software signal generator, the modulation phase remains constant during the measurement, so the PLL can be omitted here. During the data processing, the $2f$ and $1f$ signals were demodulated for intensity calibration and concentration retrieval, while the $2f$ peak position was chosen as the reference for frequency locking.

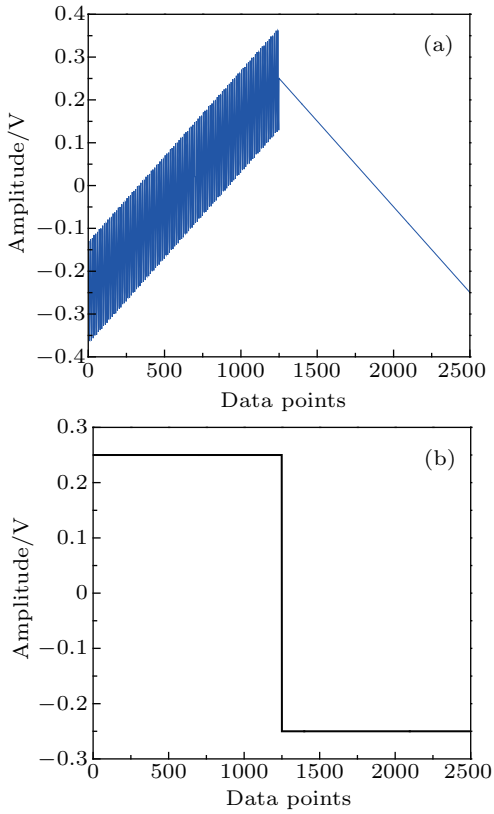


Fig. 3. Semi-modulated triangle signal generated by the software signal generator. (a) Laser current scanning signal and (b) TTL trigger signal.

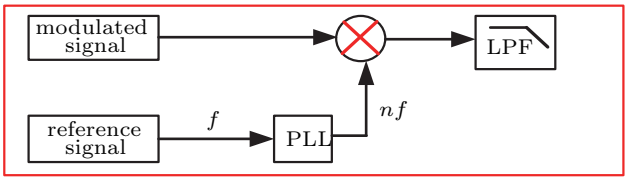


Fig. 4. Schematic diagram of the LabVIEW-based software lock-in amplifier.

(III) Frequency locking

The principle of the proposed correlation frequency locking method is schematically shown in Fig. 5. When scanning the laser current with the semi-modulated triangle waveform, the $2f$ signal can be demodulated from the rising part of the scan wave. During the measurement, the $2f$ peak position may change with the shift of the laser wavelength (Fig. 5(a)), which can be used as a reference for frequency locking.

In order to accurately identify the wavelength shift, as shown in Fig. 5(b), the correlation coefficient of the reference signal and the real signal is calculated by moving the real signal, where the moving step can be defined as an arbitrarily small length. Then the wavelength shift is determined by the maximum of the correlation coefficient (the inset of Fig. 5(b)), and the error control signal is accordingly calculated by a software PID. Finally, the operating current of the laser is adjusted in real time by communicating with the LDC-3724B through a USB cable. In particular, the proposed correlation frequency locking method still works at low signal to noise ratios and can be developed as a general method for TDLAS based applications.

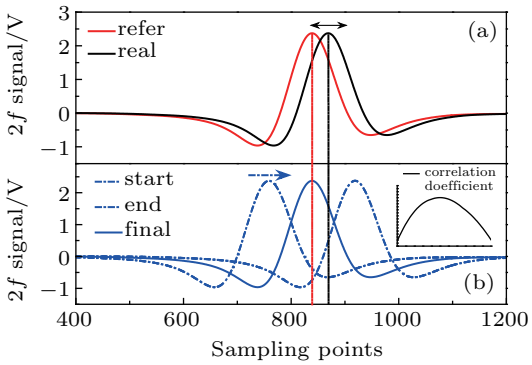


Fig. 5. Schematic diagram of the proposed method for frequency locking. (a) Wavelength shift between the refer signal and real signal. (b) The process of calculating the peak shift, the inset is the result of correlation coefficient.

3. Results and discussion

3.1. Optimization of the modulation amplitude

The relationship between the WMS-$2f$ peak height and the modulation amplitude was characterized before the N_2O concentration measurement. A 2-ppm (here the unit 1 ppm = 1.81205 mg/m^3) standard of N_2O and N_2 gases was used to optimize the modulation amplitude at a pressure of 0.1 atm. As shown in Fig. 6, the WMS-$2f$ peak height increases rapidly before reaching a maximum at a modulation amplitude of 0.25 V, and then falls slowly. Note that the optimum modulation amplitude of 0.25 V was used for all following measurements.

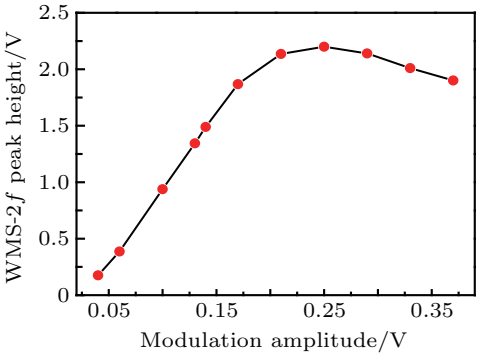


Fig. 6. The $2f$ signal of N_2O gas for different modulation amplitudes.

3.2. Static N_2O detections

In order to validate the performance of the N_2O gas detection system, a set of static N_2O detections were performed at room temperature. During the detections, a 2-ppm standard N_2O & N_2 gas was firstly diluted by pure N_2 to a range of 0.5 ppm to 2 ppm, and then the sample was pumped to a pressure of 0.1 atm. The WMS-$2f$ signals and direct absorption spectroscopy (DAS) signals at different N_2O&N_2 mixing ratios are shown in Fig. 7, where the WMS-$2f$ signals were demodulated from the rising edge signals, and the absolute concentrations values were derived from a Voigt fitting of the

falling edge signals. It should be noted that, the DAS signal is just used for the $2f/1f$ calibration during the atmospheric detection.

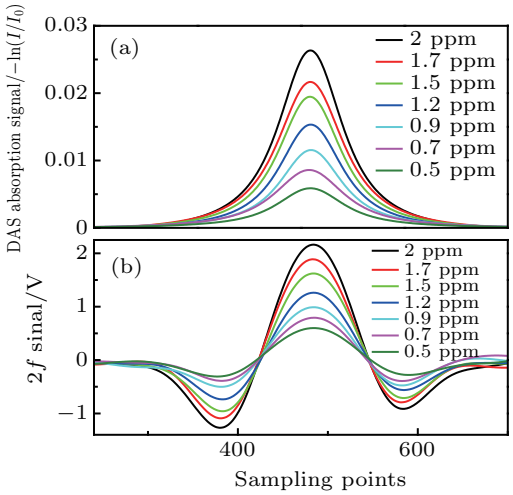


Fig. 7. Simultaneous measurements of (a) WMS-$2f$ signals and (b) DAS signals at different N_2O:N_2 mixing ratios.

The calibration-free WMS-$2f/1f$ signals are obtained by demodulating from the rising edge signal by the LabVIEW-based software lock-in amplifier. Then, comparisons between the WMS-$2f$ and WMS-$2f/1f$ methods were also studied, linear fit of the concentrations derived from the absorption spectroscopy signals to the WMS-$2f$ peak amplitude and WMS-$2f/1f$ were shown in Fig. 8, yields an R^2 value of 0.9967 and 0.9977, respectively. There were no significant differences in linearity between both methods, indicating that the system was stable during the static measurements.

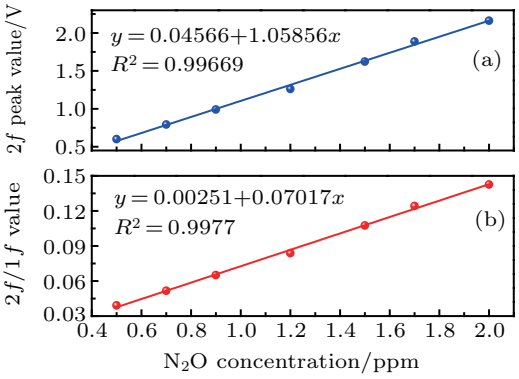


Fig. 8. Linear fit between the concentrations derived from the DAS to the WMS-$2f$ peak amplitude and WMS-$2f/1f$.

3.3. Atmospheric N_2O detections

Atmospheric N_2O detections were performed based on the WMS-$2f/1f$ method by circulating the sample in the MPC using an air pump and a pressure controller at a pressure of 0.1 atm. Figure 9 shows the continuous measurements over 5 hours with a 1-s interval (in gray), where each point is the result of 50 averages. Two smoothing method, the point-by-point exponential smoothing (in red) and the Kalman filtering (in blue), were employed to improve the precision of the system. As shown in Fig. 9, the point-by-point exponential smoothing method shows a better performance than the Kalman filtering method. During the measurement, the concentration of atmospheric N_2O varied from 295 ppb to 345 ppb, and the average concentration was around 320.5 ppb.

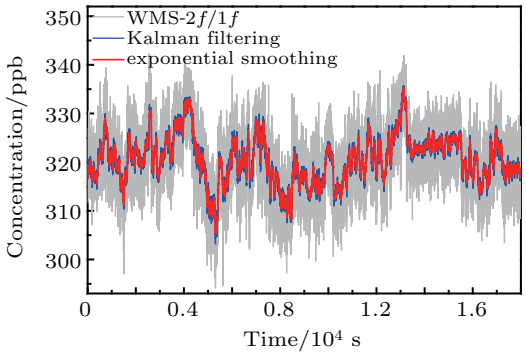


Fig. 9. Continuous measurement of atmospheric N_2O gas over 5 hours with different smoothing methods.

To further evaluate the detection limits of the system, an Allan deviation analysis was performed on the continuous time series measurements. As shown in Fig. 10, the Allan deviation analysis of the results indicates a detection limit of ~ 0.02 ppm at 1-s integration time, and the optimal detection limit is estimated to be ~ 0.005 ppm at 40-s integration time. For further improvement of the measurement precision, future works will be focused on maintaining the system temperature and choosing a more sensitive absorption line.

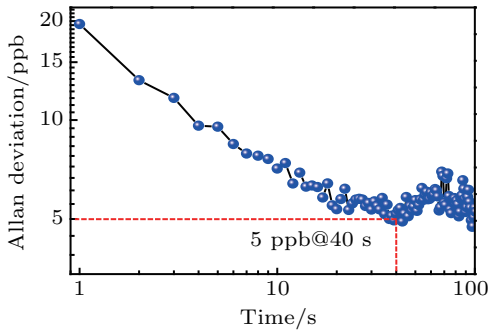


Fig. 10. Allan deviation for the time series measurement of N_2O in atmospheric air.

4. Conclusion

A compact, fast, mid-infrared atmospheric N_2O gas sensor has been developed using a 3.939-μm inter-band cascade laser and frequency locking technique. To simplify the system, a software signal generator and software lock-in amplifier were designed based on a DAQ card in the LabVIEW environment. For eliminating the absorption interference from water vapor, the working pressure was controlled at 0.1 atm by a gas pump and a pressure controller. In addition, a novel correlation frequency locking method was developed for long term trace gas detections. Finally, the analysis of the detection limit and the stability confirmed the potential of the system for long term atmospheric N_2O sensing.

References

[1] Ravishankara A R, Daniel J S and Portmann R W 2009 *Science* **326** 123

[2] Stocker T, Qin D H, Plattner K, *et al.* 2013 *Climate Change 2013: The Physical Science Basis [M]* (Cambridge: Cambridge University Press) pp. 128–130

[3] Castillo P C, Sydoryk I, Gross B and Moshary F 2013 *Chem. Biological Sensing Technol.* **8718** 87180J

[4] Baggs E M, Smales C L and Bateman E J 2010 *Biol. & Fertility Soils* **46** 793

[5] Zhang J and Han X 2008 *Atmos. Environment* **42** 291

[6] Nelson D D, McManus B, Urbanski S, Herndon S and Zahniser M S 2004 *Spectrochim. Acta Part. A: Mol. Biomolecular Spectroscopy* **60** 3325

[7] Wright S, Duxbury G and Langford N 2006 *Appl. Phys. B* **85** 243

[8] Yu Y, Sanchez N P, Griffin R J and Tittel F K 2016 *Opt. Express.* **24** 10391

[9] Cui X, Dong F, Zhang Z, Sun P, Xia H, Fertein E and Chen W 2018 *Atmos. Environment* **189** 125

[10] Dong L, Li C, Sanchez N P, Gluszek A K, Griffin R J and Tittel F K 2016 *Appl. Phys. Lett.* **108** 011106

[11] Li C, Dong L, Zheng C and Tittel F K 2016 *Sens. Actuators B: Chemical* **232** 188

[12] Ma Y, Lewicki R and Razeghi M 2013 *Opt. Express* **21** 1008

[13] Yanagawa T, Saito S and Yamamoto Y 1984 *Appl. Phys. Lett.* **45** 826

[14] Dong L, Yin W, Ma W and Jia S 2007 *Meas. Sci. Technol.* **18** 1447

[15] Gong P, Xie L, Qi X Q and Wang R 2015 *IEEE Photon. Technol. Lett.* **27** 545

[16] Wang Q, Wang Z and Ren W 2017 *Meas. Sci. Technol.* **28** 065102

[17] Wang G, Mei J, Tian X, Liu K, Tan T, Chen W and Gao X 2019 *Opt. Express* **27** 4878

[18] Wang G S, Yi H M and Cai T D 2012 *Acta Phys. Sin.* **61** 120701 (in Chinese)

[19] Goldenstein C S, Strand C L, Schultz I A, Sun K, Jeffries J B and Hanson R K 2014 *Appl. Opt.* **53** 356

[20] Sun K, Chao X and Sur R 2013 *Meas. Sci. Technol.* **24** 125203

[21] Reid J and Labrie D 1981 *Appl. Phys. B* **26** 203

[22] Hill C, Gordon I E, Kochanova R V, *et al.* 2016 *J. Quantum Spectrosc. & Radiat. Trans.* **177** 4